ISSN 0965-5441, Petroleum Chemistry, 2024, Vol. 64, No. 4, pp. 500–510. © Pleiades Publishing, Ltd., 2024.
ISSN 0965-5441, Petroleum Chemistry, 2024. © Pleiades Publishing, Ltd., 2024.

Ethylene/Propylene Copolymerization and Their Terpolymerization with 5-Ethylidene-2-norbornene over Catalytic Systems Based on Half-Sandwich Titanium Complexes with Organoaluminum and Organoboron Activators

E. E. Faingol'd[a,*], S. L. Saratovskikh[a], S. A. Zhukov[a], A. N. Panin[a], I. V. Zharkov[a], O. N. Babkina[a], N. N. Lashmanov[a], and N. M. Bravaya[a]

[a] *Federal Research Center of Problems of Chemical Physics and Medicinal Chemistry, Russian Academy of Sciences (FRC PCP MC RAS), Chernogolovka, 142432 Russia*
**e-mail: fine@cat.icp.ac.ru; fevgeny@mail.ru*

Received February 27, 2024; revised March 22, 2024; accepted April 10, 2024

Abstract—Half-sandwich titanium complexes, specifically Cp^*TiCl_3 and $Cp^*Ti[O(2,6\text{-}^iPr_2\text{-}Ph)]Cl_2$, were investigated as catalytic precursors for the synthesis of ethylene/propylene copolymers and ethylene/propylene/5-ethylidene-2-norbornene terpolymers. For this purpose, a variety of activators were tested: modified polymethylaluminoxane; boron-containing compounds such as $B(C_6F_5)_3$ and $Ph_3CB(C_6F_5)_4$ in combination with triisobutylaluminum (TIBA); isobutylaluminoxane (IBAO), and isobutylaluminum aryloxide $(2,6\text{-}^tBu_2,4\text{-Me-PhO-})Al^iBu_2$ (Al_{BHT}). In the copolymerization of ethylene and propylene, the catalysts exhibited high activity when activated by MMAO-12 and $TIBA+Ph_3CB(C_6F_5)_4$ but low activity with $TIBA+B(C_6F_5)_3$ and Al_{BHT}. With IBAO as an activator, these catalysts were found to be totally ineffective. The catalysts exhibited low activity in terpolymerization. It was further revealed that more than one type of active sites was generated in the catalytic systems: these sites were responsible for simultaneous formation of low-molecular-weight and ultrahigh-molecular-weight polymers. The composition of the copolymers as well as their thermophysical and physicomechanical properties were shown to depend on the type and composition of the catalytic system.

Keywords: ethylene/propylene copolymers, rubber, ethylene, propylene, diene, copolymerization, titanocene, activator

DOI: 10.1134/S0965544124010158

ABBREVIATIONS

Al_{BHT}—Isobutylaluminum aryloxide, $(2,6\text{-}^tBu_2,4\text{-Me-PhO-})Al^iBu_2$,
GPC—Gel permeation chromatography,
DSC—Differential scanning calorimetry,
IBAO—Isobutylaluminoxane,
XRD—X-ray diffraction analysis,
EPM—Ethylene–propylene copolymer,
EPDM—Ethylene–propylene–diene terpolymer,
Cp—Cyclopentadienyl,
Cp*—Pentamethyl cyclopentadienyl, $C_5(CH_3)_5$,
MAO—Methylaluminoxane,
MMAO-12—Modified methylaluminoxane,
P—Propylene,
TIBA—Triisobutylaluminum, Al^iBu_3,
E—Ethylene,
ENB—5-Ethylidene-2-norbornene,
M_w—Weight-average molecular weight,
M_n—Number-average molecular weight.

Ethylene–propylene (EPM) and ethylene–propylene–diene (EPDM) copolymers are elastomeric polymers widely demanded and extensively used in the automotive, rubber, and cable industries, as well as in the manufacture of construction materials, impact-resistant plastics, etc.

The production of EPM and EPDM is based solely on catalytic coordination polymerization processes. The catalyst type plays a key role in the formation of EPM and EPDM with desired compositions and molecular weights, and these parameters are critical to the operating characteristics such as microstructure, crystallinity, and glass transition temperature, as well as the molecular-weight and thermophysical properties of the products. There are various classes of catalytic systems suitable for the production of EPM and EPDM, including those produced on an industrial scale [1–3].

Constrained geometry catalysts (CGCs) contain a η^5-Cp ligand and a donor ligand (Don) linked by a bridging group. The bridging group reduces the Cp–M–Don angle (M = Ti, Zr, Hf) by about 20°–30° compared to sandwich metallocene complexes Cp–M–Cp, thus ensuring high availability of a transition metal in the active site and a high degree of comonomer incorporation (up to 20 mol % of 1-octene) [1, 4, 5]. The Don is linked to the transition metal by a σ-bond and ensures the high stability of this catalyst type at elevated temperatures (up to 160–180°C).

Non-bridged mono-Cp titanium complexes are even less sterically hindered. For example, in the copolymerization of ethylene with 1-hexene at 0 to –78°C and atmospheric pressure, with the composition of comonomers being varied, the catalytic complex $Cp^*TiMe_3/B(C_6F_5)_3$ has produced high- and ultrahigh-molecular-weight copolymers with ethylene content varying within about 5–85% (although this catalytic system exhibited moderate or even low activity) [6]. Bavarian et al. [7] investigated catalytic systems like $Cp^*TiMe_3/B(C_6F_5)_3$ in the terpolymerization of ethylene, propylene, and 5-ethylidene-2-norbornene. With moderate catalytic activity, a high-molecular-weight copolymer with up to 40 mol % propylene and up to 10 mol % diene was produced at –18°C and a total comonomer pressure of 1 atm.

Cp^*TiMe_3/MAO is one of the most efficient catalytic systems for the synthesis of syndiotactic polystyrene [8]. However, further research is needed with regard to the role of catalytic intermediates both in this type of catalysts (Ti^{II}, Ti^{III}, or Ti^{IV}) and in systems where some other activators are used. A series of NMR/EPR examinations of $Cp^*TiMe_3/B(C_6F_5)_3$, $Cp^*TiMe_3/[Ph_3C][B(C_6F_5)_4]$, and $Cp^*TiCl_{2,3}$/MAO for styrene polymerization have demonstrated that in catalytic systems of this kind, more than one type of active sites can be generated simultaneously [9, 10].

Half-sandwich non-bridged titanium complexes with donor aryloxy ligands are structurally similar to the phosphinimides, ketimides, guanidinates, iminoimidazolinates, and amidinates manufactured by ARLANXEO and extensively used for commercial rubber production [3]. These complexes, first synthesized and investigated by a research group led by Prof. Nomura in 1998 [11, 12], are now well-known as catalysts for the polymerization of ethylene as well as the copolymerization of ethylene with higher α-olefins and cyclic olefins [11–16]. The half-sandwich complexes activated by MAO and perfluorophenylborates are distinguished by high activity in polymerization and high affinity for α-olefins and cyclic olefins. The effects of organoboron activators on the catalytic performance of $Cp^*TiMe_2(O\text{-}2,6\text{-}{}^iPr_2C_6H_3)$ in the polymerization of 1-hexene were investigated in [16]. With $B(C_6F_5)_3$ as a cocatalyst, the catalytic activity in the polymerization of 1-hexene was extremely low, but it was significant in the presence of $Ph_3CB(C_6F_5)_4$. The reaction between $Cp^*TiMe_2(O\text{-}2,6\text{-}{}^iPr_2C_6H_3)$ and $B(C_6F_5)_3$ was shown to lead to catalyst decomposition and/or formation of several compounds even at –70°C, whereas no decomposition was observed in the reaction between the complex and $Ph_3CB(C_6F_5)_4$. To the best of our knowledge, available publications offer no data on the use of catalytic aryloxide titanium complexes in ethylene/propylene copolymerization or ethylene/propylene/5-ethylidene-2-norbornene terpolymerization for the synthesis of EPM or EPDM.

The purpose of the present study was to investigate and compare the catalytic performance of non-bridged titanium complexes such as Cp^*TiCl_3 and $Cp^*TiCl_2(O\text{-}2,6\text{-}{}^iPr_2C_6H_3)$ in the synthesis of bipolymers (ethylene/propylene) and terpolymers (ethylene/propylene/5-ethylidene-2-norbornene) for the production of EPM and EPDM, with organoaluminum and organoboron compounds as activators. The study was further aimed at identifying the effects of the catalyst type on the copolymerization kinetics and the copolymer properties. To activate chlorine-containing titanium complexes, we additionally used some activators specially developed in our previous studies such as

IBAO [17] and aryloxide Al_{BHT}, which is one of the series of isobutylaluminum aryloxides that exhibited high activating capacity for dimethylated metallocene precursors in the homopolymerization of ethylene and propylene, as well as in ethylene/propylene copolymerization and ethylene/propylene/5-ethylidene-2-norbornene terpolymerization [18–22].

EXPERIMENTAL

Reagents. We used high purity grade solvents that were dried and stored over 4 Å molecular sieves. Oxygen-sensitive and moisture-sensitive compounds were handled in an atmosphere of 99.998%-pure argon. Ethylene and propylene (manufactured by the Moscow Refinery, Russia) were dried by passing through a 4 Å activated molecular sieve column. Cp^*TiCl_3 (Dalchem, Russia) was used as received. MMAO-12, TIBA, $[Ph_3C][B(C_6F_5)_4]$, and $B(C_6F_5)_3$ (Sigma-Aldrich Corp., USA) were also used without pretreatment. ENB (Sigma-Aldrich Corp., USA) was dried and stored over 4 Å molecular sieves.

Synthesis of $Cp^*TiCl_2(O\text{-}2,6\text{-}{}^iPr_2C_6H_3)$. This complex was synthesized in accordance with the modified procedure described in [11]. Cp^*TiCl_3 was mixed with phenol ($OH\text{-}2,6\text{-}{}^iPr_2C_6H_3$) in toluene at a molar ratio of 1 : 2.5. The reaction was carried out by stirring the resultant solution at 70°C for 5 h. To remove the evolved HCl, the reaction solution was bubbled with argon. The reaction completeness was monitored by ^1H NMR spectroscopy. A red powder was prepared by distilling off toluene and was recrystallized in a dichloromethane/heptane (1 : 3) solvent mixture at 5°C to obtain needle-like red crystals of the target complex.

^1H NMR $Cp^*TiCl_2(O\text{-}2,6\text{-}{}^iPr_2C_6H_3)$ ($CDCl_3$, δ, ppm): 1.22 (d, 12H, $(CH_3)_2CH$–), 2.18 (s, 15H ($C_5(CH_3)_5$)), 3.17 (m, 2H $(CH_3)_2CH$–), (d, 1H, Ar-H), (t, 2H, Ar-H).

Synthesis of IBAO. IBAO was synthesized by controlled hydrolysis of TIBA [17]. A toluene solution of TIBA precooled to –78°C was added to a specific amount of water (free of dissolved air) based on an Al/H_2O molar ratio of 2 : 1. The resultant mixture was stirred for 15 min, then slowly heated to room temperature for 40 min. The total hydrolysis time was 1 h. The IBAO was prepared 2 h before the polymerization.

Synthesis of Al_{BHT}. Aryloxide (Al_{BHT}) was synthesized in accordance with the procedure we previously described in [18].

Copolymerization of ethylene and propylene. The copolymerization was carried out in a 200 mL stainless steel reactor. The reactor was evacuated at 50°C for 1 h, filled with argon, and cooled to room temperature. A vial with a weighed sample of the appropriate titanium complex (catalyst precursor) was placed in the reactor under an argon flow. The reactor was evacuated and, after introducing a toluene solution of the activator, heated to 30°C. The calculated amounts of first propylene and then ethylene were successively injected to achieve an E/P molar ratio of 0.7 : 1 in the solution and a specific monomer pressure in the gas phase. The catalyst was introduced into the solution by crushing the sample vial to initiate the polymerization. A constant pressure was maintained by adding ethylene. The reaction was terminated by introducing a 5% ethanol solution of HCl into the reactor. The polymer was washed with a water/ethanol mixture, filtered, and dried at 60°C in a vacuum oven to constant weight.

Terpolymerization of ethylene, propylene, and 5-ethylidene-2-norbornene. For the ternary copolymerization of ethylene, propylene, and 5-ethylidene-2-norbornene, we followed the same procedure as for the ethylene/propylene copolymerization except that the required amount of 5-ethylidene-2-norbornene was introduced into the reactor simultaneously with the toluene solution of the activator.

Characterization of copolymers. Specimens of copolymers were analyzed by GPC, DSC, IR spectroscopy, and XRD.

The gel chromatograms of the specimens were recorded on a Waters GPCV 2000 chromatograph using a PLgel 5 μm MIXED-C column in 1,2,4-trichlorobenzene at 135°C. The molecular weights of the copolymers were evaluated based on the universal calibration curve taking into account the constants K and α from the Mark–Houwink equation for polystyrene and polyethylene in 1,2,4-trichlorobenzene.

The melting point and specific heat of fusion of the copolymers were derived from DSC data. The DSC measurements were performed on a DSC 822E calorimeter (Mettler Toledo, Switzerland) using STARe 15 software. The thermograms were recorded through three heating–cooling–heating cycles in an inert atmosphere with the temperature being varied between –100 and +170°C at a rate of 10°C/min. Table 1 presents

the characteristic melting points and thermal effects of melting transitions for the second heating.

The copolymer compositions were derived from the IR spectra of polymer films in accordance with the procedures described in [23, 24] using a PerkinElmer Spectrum 100 FTIR spectrometer.

The XRD patterns of copolymer films were recorded on an ARLX'TRA diffractometer (Thermo Fisher Scientific, Switzerland) equipped with a solid-state detector using θ–θ geometry in the 5°–60° with a step of 0.2°/min and a counting time of 1 s/step.

Stress–strain testing of polymer specimens. The stress–strain tests of the copolymer specimens were run using a 2166 P-5 Plastics Testing Machine at room temperature in accordance with ISO 37 (Dietype 1). The strain rate was 10 mm/min. The physicomechanical properties of the specimens were determined by averaging the test data for five copolymer specimens. The elongation at break (EL) of the copolymers was evaluated by the formula: $EL = (l_1 - l_0)/l_0 \times 100$, where l_1 is the length of the broken specimen measured by summing the lengths of the two fragments being merged; and l_0 is the initial length of the specimen.

RESULTS AND DISCUSSION

The titanium complexes used in this investigation of ethylene/propylene (binary) and ethylene/propylene/5-ethylidene-2-norbornene (ternary) catalytic copolymerization are schematically illustrated below:

Catalytic properties of Ti–Cl and Ti–1 in binary and ternary copolymerization using various activators.

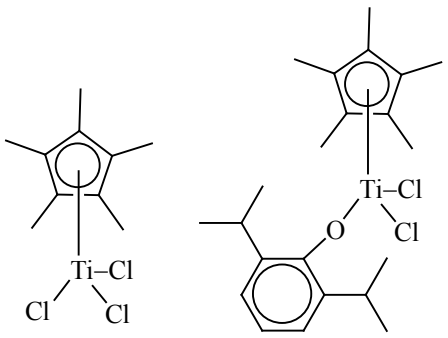

Ti–Cl **Ti–1**

Copolymer properties. The catalytic properties of **Ti–Cl** and **Ti–1** in ethylene/propylene copolymerization and ethylene/propylene/5-ethylidene-2-norbornene terpolymerization using various activators, as well as the properties of the copolymers produced are summarized in Table 1.

When **Ti–Cl** was activated by MMAO-12 ($[(CH_3)_{0.95}(n\text{-}C_8H_{17})_{0.05}AlO]_n$), the activity of this catalytic system in ethylene/propylene copolymerization (run 1) was 192 kg of the copolymer per mole of titanium per hour per atmosphere pressure ($kg_{polymer}\, mol_{Ti}^{-1}\, h^{-1}\, atm^{-1}$). At a comonomer molar ratio of 0.7 : 1 in the reaction medium, the copolymer contained about 7 mol % of propylene. During the terpolymerization at a comonomer molar ratio of 4.7 : 4.3 : 1 (run 2), with other conditions being equal, an almost five-fold drop in the activity was observed. This could be associated with diene reactivity, which is lower than that of propylene, and/or with possible catalyst deactivation reactions. Despite the lower propylene to ethylene molar ratio in the reaction medium in the terpolymerization case (0.91 versus 1.43 for copolymerization), the propylene content in the copolymer increased to 10.5 mol %. The diene content was about 1 mol %. When **Ti–Cl** was activated by TIBA+$Ph_3CB(C_6F_5)_4$, the catalytic activity in copolymerization (run 3) was about double that with MMAO-12, but it dropped by a factor of more than ten in terpolymerization (run 4). The propylene content was about 9.3 mol % in the bipolymer and about 7.3 mol % in the terpolymer, roughly consistent with the decrease in its ratio to ethylene in the initial solution. The **Ti–Cl** catalytic system with bulk activators (borate and MMAO) provided a markedly lower incorporation of diene, probably due to the more strong steric limitations for the entrance of diene into active sites. A similar pattern was observed in terpolymerization over Cp*$TiMe_3$/$B(C_6F_5)_3$ at low temperatures [7]. Furthermore, similar diene effects in terpolymerization (specifically, an about 10-fold drop in terpolymerization activity after diene introduction) were reported when metallocene catalysts were activated by MAO [25] or by TIBA+borate [26].

The kinetic curves of copolymerization and terpolymerization over **Ti–Cl**/MMAO-12 and **Ti–Cl**/TIBA+$Ph_3CB(C_6F_5)_4$ are shown in Fig. 1. In the presence of diene, the most pronounced deactivation was observed for the catalytic system with the borate activator.

In ethylene/propylene copolymerization over **Ti–Cl**/TIBA+$Ph_3CB(C_6F_5)_4$, a homogeneous copolymer

Table 1. E/P copolymerization and E/P/ENB terpolymerization over Ti–Cl/activator and Ti–1/activator (reaction conditions: toluene as a solvent; 60 mL; 30°C; E/P = 0.7 : 1; E/P/ENB = 4.7 : 4.3 : 1)

Run no.	Catalyst	Activator	Monomers	[Ti], μmol	*t*, min	A[a]	M_w[b]	M_w/M_n	P/ENB[c]	T_{melt},[d] °C	ΔH,[e] J/g	χ,[h] %	*D*,[i] nm	σ_b,[j] MPa	ε_b,[k] %
1	**Ti–Cl**	MMAO-12 Al/Ti = 1000	E/P	7.95	18	192	17[f] (88%)	1.9	7.3/0	87; 113; 123	53	54.1	10	2.6	5
2	**Ti–Cl**	MMAO-12 Al/Ti = 1000	E/P/ENB	9.67	47	41	25[f] (70%)	3.9	10.5/1.2	86; 123	35.8	42.7	14	6.0	57
3	**Ti–Cl**	TIBA + $Ph_3CB(C_6F_5)_4$	E/P	5.53	15.5	370	55	2.2	9.3/0	85; 119	57.6	36.2	14	4.4	460
4	**Ti–Cl**	TIBA + $Ph_3CB(C_6F_5)_4$	E/P/ENB	8.29	67.4	29	31[f] (51%)	3.6	7.3/0.3	89; 120	39.3	37.2	14	11.0	150
5	**Ti–1**	MMAO-12 Al/Ti = 1000	E/P	5.57	5.7	2050	821[f,g] (56%) 55 (44%)	2.8 1.7	19.7/0	100; 115	25	26.4	9	1.3	290
6	**Ti–1**	MMAO-12 Al/Ti = 1000	E/P/ENB	4.87	60	62	1391[f,g] (36%) 75 (64%)	2.7 1.7	13.9/2	60	11	19.8	8	9.1	450
7	**Ti–1**	TIBA + $Ph_3CB(C_6F_5)_4$ Al/Ti = 300 B/Ti = 1	E/P	6.73	4.5	2200	100[f] (53%) 62 (47%)	2.7 1.7	11/0	107; 124	54.8	29.7	18	1.9	46
8	**Ti–1**	TIBA + $Ph_3CB(C_6F_5)_4$ Al/Ti = 300 B/Ti = 1	E/P/ENB	4.87	90	1	–	–	12/1	47; 93; 123		–	–	–	
9	**Ti–1**	TIBA + $B(C_6F_5)_3$ Al/Ti = 300 B/Ti = 1	E/P	9.74	35	74	–	–	19/0	101	6.6	22.4	7	0.8	360
10	**Ti–1**	TIBA + $B(C_6F_5)_3$ Al/Ti = 300 B/Ti = 5	E/P	9.04	36	59	181	3.7	6/0	95; 124	8	16.9	9	0.5	770
11	**Ti–1**	TIBA + $B(C_6F_5)_3$ Al/Ti = 300 B/Ti = 1	E/P/ENB	8.23	41	13	–	–	13/2.7	93; 125	16.4	33.7	14	7.6	550
12	**Ti–1**	Al_{BHT} Al/Ti = 300	E/P	8.81	55	9	–	–	9.4/0	91; 123	4	4	12	4.9	520
13	**Ti–1**	IBAO Al/Ti = 300	E/P	4.63	60	–	–	–	–	–	–	–			

[a] Activity (in $kg_{polymer}\ mol_{Ti}^{-1}\ h^{-1}\ atm^{-1}$).
[b] Weight-average molecular weight of copolymer's soluble fraction (kg/mol).
[c] P/ENB in copolymer (mol %).
[d] Derived from the melting peak maximum during the second heating of specimens after recrystallization.
[e] Specific heat of fusion.
[f] Given that the specimens were dissolved incompletely, % of the soluble fraction relative to the total polymer weight is indicated in parentheses.
[g] The MWD curve has two peaks. The contribution of each component is indicated in parentheses.
[h] Crystallinity was evaluated as the ratio between the integrated intensity areas of the crystalline and amorphous phases (based on XRD data).
[i] Average crystallite size (based on XRD data).
[j] Tensile stress.
[k] Breaking elongation.

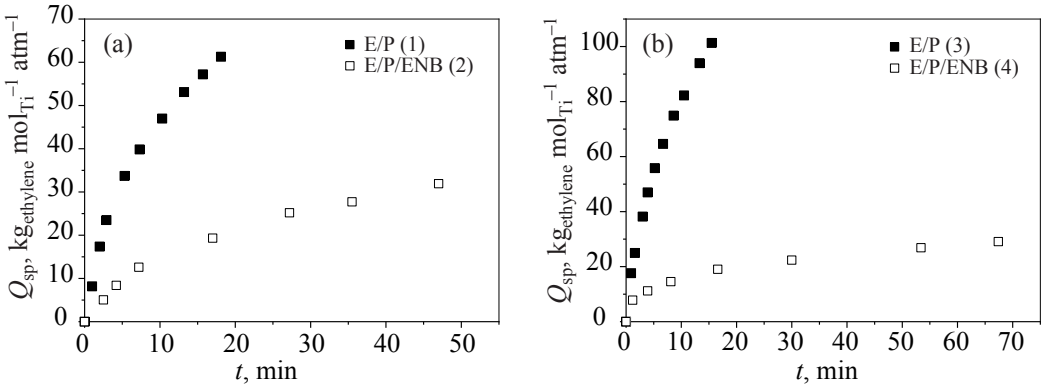

Fig. 1. Specific ethylene consumption (Q_{sp}) over time using **Ti–Cl** activated by MMAO-12 and TIBA+$Ph_3CB(C_6F_5)_4$ in binary and ternary copolymerization: (a) MMAO-12/$Ph_3CB(C_6F_5)_4$; and (b) TIBA+$Ph_3CB(C_6F_5)_4$. The curve numbers correspond to the run numbers in Table 1.

with M_w = 55 000 and a narrow polydispersity index (M_w/M_n = 2.2) was produced (run 3). Activation by MMAO-12 resulted in the formation of a copolymer partially soluble (88%) under GPC conditions with M_w = 17 000 and a low polydispersity index (M_w/M_n = 1.9, run 1). The insoluble ultrahigh-molecular-weight fraction of the copolymer was formed on active sites of a different type, likely resulting from transformation of the titanium cation complex during the copolymerization. In terpolymerization over **Ti–Cl** activated both by MMAO-12 and TIBA+$Ph_3CB(C_6F_5)_4$, the copolymers had higher heterogeneity (with soluble fractions accounting for 70 and 51%, respectively). These terpolymers exhibited higher molecular weights of soluble fractions and higher polydispersity indices than the binary copolymers (runs 2 and 4). Figure 2 presents the molecular weight distribution (MWD) curves of the soluble fractions of the binary and ternary copolymers produced using **Ti–Cl** with various activators. Metallocene catalysts activated by MAO and TIBA+borate are known to promote the formation of homogeneous copolymers with low polydispersity indices [24, 25]. This suggests that, in the catalytic systems under study, the titanium complex was transformed with the generation of various active sites responsible for the formation of low-molecular-weight and high-molecular-weight copolymers.

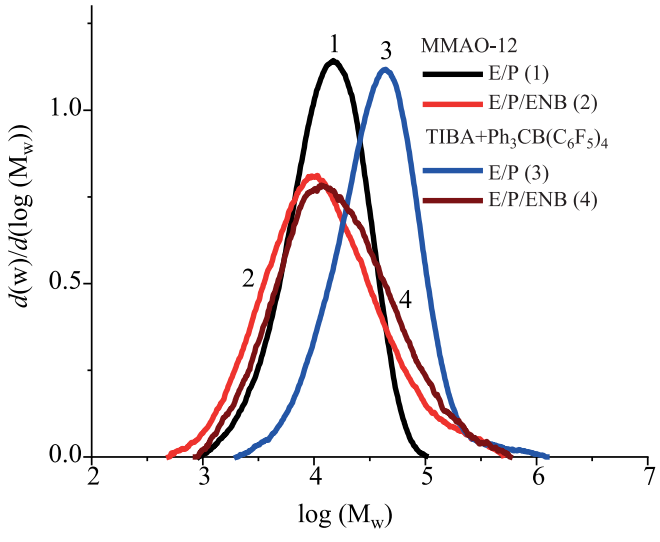

Fig. 2. MWD curves of soluble fractions of bipolymers and terpolymers produced using **Ti–Cl** with various activators. The curve numbers correspond to the run numbers in Table 1.

A comparison of the plots in Figs. 1 and 3, in combination with the data of Table 1, shows that, both with MMAO-12 and TIBA+$Ph_3CB(C_6F_5)_4$ as activators, **Ti–1** exhibited very high activity in the copolymerization of ethylene and propylene. The activity of **Ti–1** exceeded that of **Ti–Cl** (other conditions being equal) by more than an order of magnitude (runs 5 and 7 vs. runs 1 and 3 in Table 1). Moreover, the complex with the aryloxide ligand exhibited a noticeably better stability during copolymerization (Fig. 3). When activated by TIBA+$B(C_6F_5)_3$, both the activity and stability of the system were extremely low, consistent with the behavior of its methylated analogue, Cp*$TiMe_2$(O-2,6-$^i Pr_2C_6H_3$), previously demonstrated in the polymerization of 1-hexene with similar activation [16]. The **Ti–1** catalyst

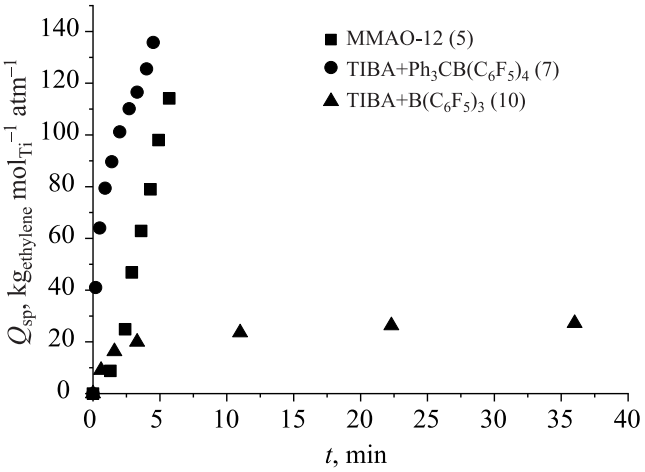

Fig. 3. Specific ethylene consumption (Qsp) over time using **Ti–1** activated by MMAO-12, TIBA+$Ph_3CB(C_6F_5)_4$, and TIBA+$B(C_6F_5)_3$. The curve numbers correspond to the run numbers in Table 1.

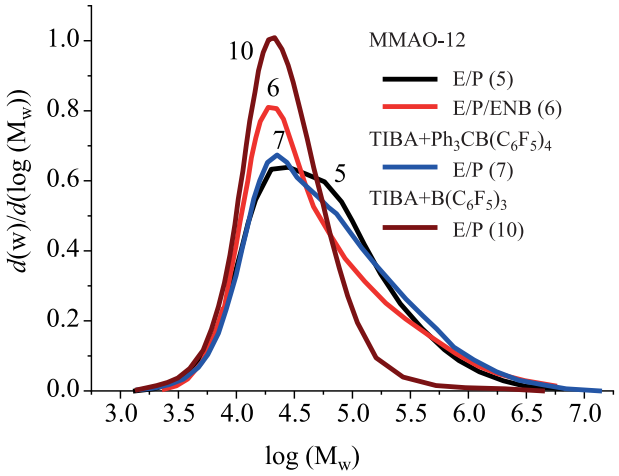

Fig. 4. MWD curves of copolymers produced using **Ti–1** with various activators. The curve numbers correspond to the run numbers in Table 1.

also exhibited very poor activity in terpolymerization. In binary copolymerization, the complex with the aryloxide ligand clearly provided a markedly higher degree of propylene incorporation than **Ti–Cl** (cf. run 2 (7.3% P) vs. run 5 (19.7% P) and run 4 (9.3% P) vs. run 7 (11.0% P), see Table 1). The **Ti–1** catalytic systems with the activators known to be effective for dimethylated metallocenes, specifically Al_{BHT} [18, 21] and IBAO [17], were tested in ethylene/propylene copolymerization. As a result, the catalyst exhibited low activity in combination with Al_{BHT} and turned out to be totally ineffective with IBAO (runs 12 and 13 in Table 1). The poor performance of the activators can likely be explained by the fact that they are able to activate only alkylated metal complexes.

A distinctive feature of copolymers produced over **Ti–1** activated by MMAO-12 and TIBA+$Ph_3CB(C_6F_5)_4$ is the bimodality of their GPC curves. As noted above, the copolymers obtained using **Ti–Cl** were likewise marked with fractional heterogeneity, i.e., the presence of an insoluble ultrahigh-molecular-weight fraction (runs 1, 2, and 4 in Table 1). In the case of **Ti–1**, the copolymer specimens were completely dissolved in 1,2,4-trichlorobenzene (TCB) at 135°C. Figure 4 illustrates the GPC data for some copolymers. The peak resolution and fractional composition are indicated in Table 1. The data of Fig. 4 and Table 1 clearly show that bulk activators such as MMAO-12 and $Ph_3CB(C_6F_5)_4$ promoted the formation of bimodal copolymers with polydispersity indices of about 2.0 for each peak. This serves as evidence of two different types of active sites, one being responsible for the formation of a high-molecular-weight polymer (with M_w of nearly 1×10^6 g/mol) and the other for the formation of a low-molecular-weight polymer (M_w ranging between 33×10^4 and 45×10^4 g/mol). The contribution of each peak is indicated in Table 1.

Figure 5 illustrates the differential fractional compositions of the ethylene/propylene copolymers produced using **Ti–1** with various activators. Interestingly, the contribution of low-molecular-weight fractions, namely Fraction 4 ($M_w = 5\times10^4$–1×10^5 g/mol) and Fraction 5 (1×10^4–5×10^4 g/mol), was significantly greater for the copolymer in run 10 (see Table 1). This was the case with stronger bounded $B(C_6F_5)_3$-based counterions that provided the lowest propylene incorporation (6 mol %). Fraction 3 was predominant, with its content being similar (1×10^5–5×10^5 g/mol) in all three copolymers. The copolymers synthesized with the bulk activators MMAO-12 and $Ph_3CB(C_6F_5)_4$ had similar content of high-molecular-weight fractions: 1×10^6–1×10^7 g/mol for Fraction 1 and 5×10^5–1×10^6 g/mol for Fraction 2, far in excess of the content of the same fractions in the copolymer obtained with $B(C_6F_5)_3$. Bearing in mind the considerable loss of activity (by a factor of about 35) and propylene incorporation capacity, these data indicate that the probability of chain transfer to **Ti–1**/$B(C_6F_5)_3$ active sites was markedly higher than in the cases of less strong bounded counterions.

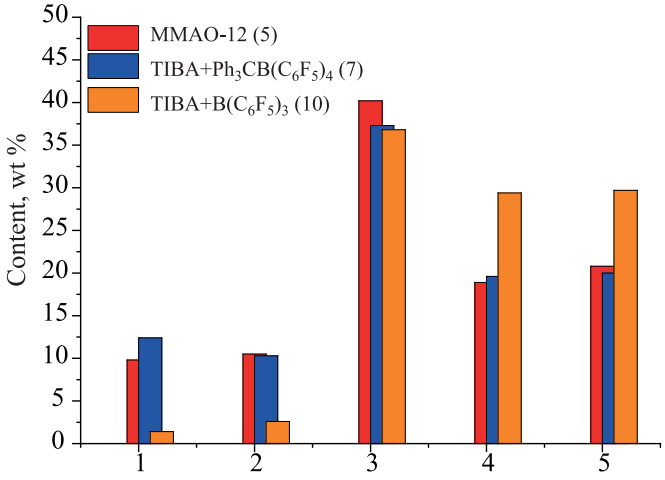

Fig. 5. Content of fractions soluble under GPC conditions in E/P copolymers produced using **Ti–1** with various activators. Fractions (M_w range, g/mol): (1) 1×10^6–1×10^7; (2) 5×10^5–1×10^6; (3) 1×10^5–5×10^5; (4) 5×10^4–1×10^5; and (5) 1×10^4–5×10^4. The copolymer numbers correspond to the run numbers in Table 1.

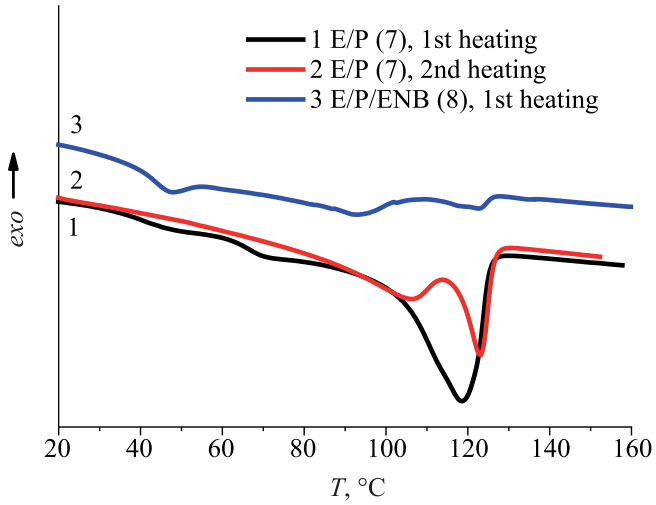

Fig. 6. Thermograms of E/P and E/P/ENB copolymers produced using **Ti–1**/TIBA+$Ph_3CB(C_6F_5)_4$ (runs 7 and 8 in Table 1).

It is worth noting that the heterogeneity of most copolymers was manifested not only in the GPC data but also in the thermophysical properties. The first-heating DSC curves mostly contained several endothermic peaks (Fig. 6). The peak intensity was markedly lower for terpolymers (except for run 11). During recrystallization (the second DSC heating), the number of peaks was reduced due to the disappearance of low-temperature peaks. The melting points (column "T_{melt}" in Table 1) were derived from the maxima of endothermic peaks after recrystallization. The specific heat of fusion (column 'ΔH' in Table 1) was evaluated based on the total heat effect.

The crystallinity (column "χ" in Table 1), determined as the ratio between the XRD-measured intensities of the crystalline and amorphous phases, was higher (up to 54%) in the **Ti–Cl**-catalyzed copolymerization cases. Intriguingly, among the copolymers produced in the presence of **Ti–Cl**, the specimens with low molecular weights and small content of the insoluble (ultrahigh-molecular-weight) fraction had greater crystallinity, likely due to a greater mobility of low-molecular-weight chains involved in recrystallization.

The crystallite sizes (column "D" in Table 1) were derived from the XRD spectra using the Scherrer equation. We clearly see that they are small and independent of the crystallinity. Below it is demonstrated that neither crystallinity nor crystallite size are decisive factors for the physicomechanical properties of these copolymers.

The copolymers obtained using **Ti–1**, which also exhibited fractional heterogeneity although they lacked an ultrahigh-molecular-weight fraction, possessed a markedly lower crystallinity (about 20–30%). The only exception was that in the cases of adding boranes to **Ti–1** (runs 9 to 11, Table 1), the crystallinity substantially increased when diene was introduced into the polymer chain (Fig. 7). This affected the strength properties of the terpolymers.

The stress–strain curves and physicomechanical properties of the copolymers are provided in Fig. 8 and Table 1. We see that, in the initial strain region, the copolymers produced using **Ti–Cl** (and distinguished by 40–60% crystallinity compared to 20–30% in the specimens obtained over **Ti–1**) generally exhibited a higher elastic modulus. The initial elastic strain regions of the copolymers obtained with **Ti–1** depended on various factors such as copolymer type, crystallinity, and catalytic system. The only exception was the ethylene/propylene copolymer obtained over **Ti–Cl**/MMAO-12 (run 1). The specimen with the lowest content of the GPC-insoluble fraction (12%), the lowest molecular weight (M_w = 17.000), and the highest crystallinity (54%) was broken without reaching the yield stress at a strain of about 5%. The terpolymer produced with

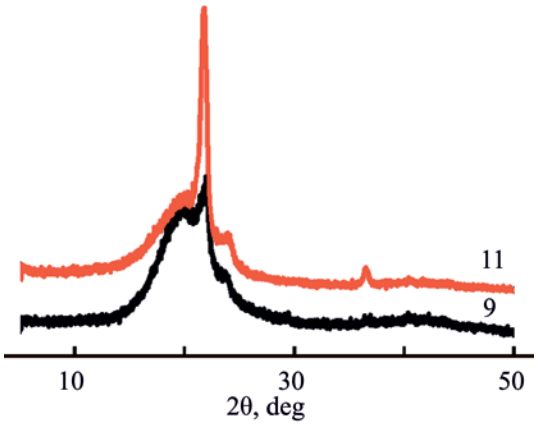

Fig. 7. XRD patterns of E/P and E/P/ENB copolymers produced using **Ti–1**/TIBA+$B(C_6F_5)_3$ (runs 9 and 11 in Table 1).

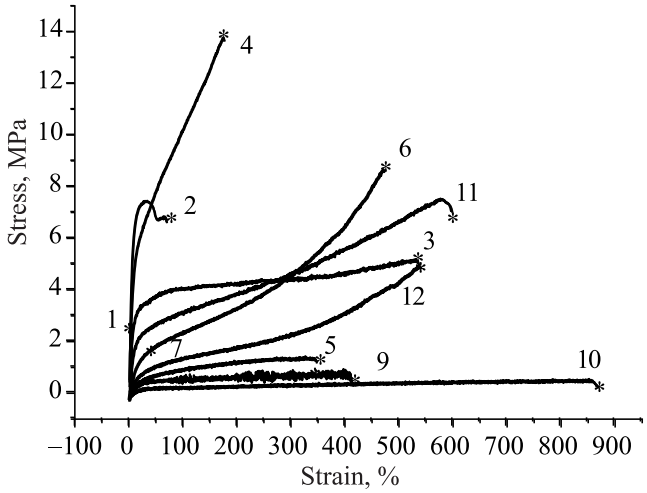

Fig. 8. Stress–strain curves of copolymers and terpolymers produced over **Ti–Cl** and **Ti–1** with various activators. The curve numbers correspond to the run numbers in Table 1.

the same catalytic system (run 2: soluble fraction 70%; M_w = 25 000; crystallinity 43%) reached a yield stress of 7 MPa at a strain of 36%, but further increasing the strain caused brittle fracturing. The other copolymers remained elastic even when the strain reached above the yield stress; their properties depended on the copolymer type, crystallinity, and catalytic system (see their σ_b and ε_b values in Table 1).

Introducing diene into the reaction mixture had a major effect on the stress–strain curves. In all cases with both catalysts, it improved the strength properties of the copolymers (runs 3 and 4). The appearance of or increasing the content of an insoluble fraction in the copolymers obtained using **Ti–Cl** increased the tensile stress (runs 2 vs. 4) and decreased the elongation at break (runs 3 vs. 4).

Ti–1 promoted the formation of completely soluble polymers. The stress–strain curves of the terpolymers produced over **Ti–1** with MMAO-12 and boron-containing activators (runs 6 and 11) are similar in shape to those of elastomers, with the tensile elongation at break (EL) being about 190% and about 300%, respectively. Increasing the B/Ti ratio (runs 9 and 10) also affected the mechanical properties: these binary copolymers exhibited breaking elongations up to 770%.

Finally, it should be noted that some other activators such as IBAO [17] and isobutylaluminum aryloxides [18, 19], known to be effective for dimethylated metallocene complexes, exhibited inadequate performance in the catalytic systems that contained the half-sandwich titanium complexes under study. No copolymers were formed over these catalytic systems with IBAO. The ethylene/propylene copolymer obtained over **Ti–1** activated by Al_{BHT} exhibited elastomeric properties to a greater extent. At low crystallinity (below 10%), the copolymer exhibited a low yield stress and fairly high strength properties, with the tensile elongation at break being about 180%. This behavior of the polymer can likely be explained by the large number of chain entanglements in the amorphous portion of the polymer.

The present study demonstrated that the use of various half-sandwich titanium complexes with various organoaluminum and organoboron activators in binary and, especially, ternary copolymerization offers an opportunity to produce copolymers with a wide range of properties. We expect that further research will be focused on the synthesis and characterization of the catalytic properties of new half-sandwich titanium complexes with the aryloxy moieties of ligands being varied. Further research should also investigate the effects of copolymerization conditions (e.g., activator type, comonomers ratio, temperature, etc.) on the production of EPM and EPDM that would satisfy the desired operating characteristics.

CONCLUSIONS

This study investigated ethylene/propylene copolymerization and ethylene/propylene/5-ethylidene-2-norbornene terpolymerization over half-

sandwich titanium complexes Cp*$TiCl_3$ (**Ti-Cl**) and Cp*$TiCl_2$(O-2,6-$^i Pr_2C_6H_3$) (**Ti-1**) with various activators, such as MMAO-12, TIBA+$Ph_3CB(C_6F_5)_4$, TIBA+$B(C_6F_5)_3$, isobutylaluminoxane, and isobutylaluminum aryloxide. The activity of **Ti–Cl** activated by TIBA+$Ph_3CB(C_6F_5)_4$ was double that with MMAO-12; in contrast, **Ti–1** exhibited comparable activity for both activator types. In binary copolymerization, **Ti–1** proved to be more stable than **Ti–Cl** with both activators. In terpolymerization, all the catalytic systems exhibited an order of magnitude lower activity than in binary copolymerization. In combination with (2,6-$^t Bu_2$, 4-Me-PhO-)Al$^i Bu_2$ (otherwise referred to as Al_{BHT} and known to be an effective for dimethylated metallocene activator), **Ti–1** exhibited low activity in binary copolymerization; this complex was totally ineffective when activated by IBAO. The copolymers obtained over both catalytic complexes activated by MMAO-12 and boron-containing activators were characterized by fractional heterogeneity (i.e., an ultrahigh-molecular-weight copolymer and a low-molecular-weight copolymer being formed simultaneously), bimodal molecular weight distribution curves, and multimodal peaks in DSC thermograms. This serves as evidence of more than one type of active sites generated in the catalytic systems.

These findings show the potential for further research to achieve the following goals: to synthesize and characterize the catalytic properties of new half-sandwich titanium complexes with the aryloxy moieties of ligands being varied; to determine the underlying causes of the multimodal properties of the copolymers; to assess the feasibility of the activation of methylated complexes by IBAO and isobutylaluminum aryloxides; and to optimize copolymerization conditions (activator type, comonomers ratio, temperature, etc.) for the production of EPM and EPDM that would satisfy the desired operating characteristics.

AUTHOR INFORMATION

E.E. Faingol'd, ORCID: https://orcid.org/0000-0002-3332-3741

S.L. Saratovskikh, ORCID: https://orcid.org/0000-0002-2419-807X

S.A. Zhukov, ORCID: https://orcid.org/0009-0005-0624-1280

A.N. Panin, ORCID: https://orcid.org/0000-0002-6279-5975

I.V. Zharkov, ORCID: https://orcid.org/0000-0001-6355-923X

O.N. Babkina, ORCID: https://orcid.org/0000-0001-7803-5965

N.N. Lashmanov, ORCID: https://orcid.org/0009-0000-2598-3873

N.M. Bravaya, ORCID: https://orcid.org/0000-0001-7773-5521

FUNDING

This work was supported by the Ministry of Science and Higher Education of the Russian Federation within governmental order (project no. 124013000722-8).

CONFLICT OF INTEREST

The authors declare no conflict of interest requiring disclosure in this article.

REFERENCES

1. Baier, M.C., Zuideveld, M.A., and Mecking, S., *Angew. Chem. Int. Ed*., 2014, vol. 53, pp. 9722–9744. https://doi.org/10.1002/anie.201400799
2. Klosin, J., Fontaine, P.P., and Figueroa, R., *Acc. Chem. Res.*, 2015, vol. 48, pp. 2004–2016. https://doi.org/10.1021/acs.accounts.5b00065
3. Bravaya, N.M., Faingol'd, E.E., Sanginov, E.A., and Badamshina, E.R., *Catalysts*, 2022, vol. 12, pp. 704–718. https://doi.org/10.3390/catal12070704
4. Stevens, J.C., Timmers, F.J., Wilson, D.R., Schmidt, G.F., Nickias, P.N., Rosen, R.K., Knight, G.W., and Lai, S.-Y., Patent EP 0416815 A2, 1991.
5. Braunschweig, H. and Breitling, F.M., *Coord. Chem. Rev*., 2006, vol. 250, pp. 2691–2720 https://doi.org/10.1016/j.ccr.2005.10.022
6. Murray, M.C. and Baird, M.C., *J. Polym. Sci., Part A: Polym. Chem*., 2000, vol. 38, pp. 3966–3976. https://doi.org/10.1002/1099-0518(20001101)38:21<3966::AID-POLA140>3.0.CO,2-4
7. Bavarian, N., Baird, M.C., and Parent, J.S., *Macromol. Chem. Phys*., 2001, vol. 202, pp. 3248–3252. https://doi.org/10.1002/1521-3935(20011101)202:17<3248::AID-MACP3248>3.0.CO,2-L
8. Tomotsu, N., Ishihara, N., Newman, T.H., and Malanga, M.T., *J. Mol. Catal. A: Chem*., 1998, vol. 128, pp. 167–190. https://doi.org/10.1016/S1381-1169(97)00171-4

9. Williams, E.F., Michael C. Murray, M.C., and Baird, M.C., *Macromolecules*, 2000, vol. 33, pp. 261–268. https://doi.org/10.1021/ma991006f
10. Bryliakov, K.P., Semikolenova, N.V., Zakharov, V.A., and Talsi, E.P., *J. Organomet. Chem*., 2003, vol. 683, pp. 23–28. https://doi.org/10.1016/S0022-328X(03)00232-8
11. Nomura, K., Naga, N., Miki, M., Yanagiand, K., and Imai, A., *Organometallics*, 1998, vol. 17, pp. 2152–2154. https://doi.org/10.1021/om980106r
12. Nomura, K., Naga, N., Mikiand, M., and Yanagi, K., *Macromolecules*, 1998, vol. 31, pp. 7588–7597. https://doi.org/10.1021/ma980690f
13. Nomura, K., Liu, J., Padmanabhan, S., and Kitiyanan, B., *J. Mol. Catal. A: Chem*., 2007, vol. 267, pp. 1–29. https://doi.org/10.1016/j.molcata.2006.11.006
14. Zhao, W. and Nomura, K., *Catalysts*, 2016, vol. 6, pp. 175–182. https://doi.org/10.3390/catal6110175
15. Zhao, W., Yan, Q., Tsutsumi, K., and Nomura, K., *Organometallics*, 2016, vol. 35, pp. 1895–1905. https://doi.org/10.1021/acs.organomet.6b00242
16. Nomura, K. and Fudo, A., *Inorg. Chim. Acta*, 2003, vol. 345, pp. 37–43. https://doi.org/10.1016/S0020-1693(02)01371-3
17. Bravaya, N.M., Panin, A.N., Faingol'd, E.E., Saratovskikh, S.L., Babkina, O.N., Zharkov, I.V., and Perepelitsina, E.O., *Polym. Bull*., 2016, vol. 73, pp. 473–491. https://doi.org/10.1007/s00289-015-1505-2
18. Faingol'd E.E, Bravaya, N.M., Panin, A.N., Babkina, O.N., Saratovskikh, S.L., and Privalov, V.I., *J. Appl. Polym. Sci*., 2015, vol. 133, pp. 43276. https://doi.org/10.1002/app.43276
19. Faingol'd, E.E., Zharkov, I.V., Bravaya, N.M., Panin, A.N., Saratovskikh, S.L., Babkina, O.N., and Shilov, G.V., *J. Organomet. Chem*., 2018, vol. 871, pp. 86–95. https://doi.org/10.1016/j.jorganchem.2018.07.001
20. Faingol'd E.E, Saratovskikh, S.L., Panin, A.N., Babkina, O.N., Zharkov, I.V., Garifullin, N.O., Shilov, G.V., and Bravaya, N.M., *Polymers*, 2021, vol. 220, p. 123559. https://doi.org/10.1016/j.polymer.2021.123559
21. Faingol'd, E.E., Saratovskikh, S.L., Panin, A.N., Babkina, O.N., Zharkov, I.V., Kapasharov, A.T., Bubnova, M.L., Shilov, G.V., and Bravaya, N.M., *Polymers*, 2023, vol. 15, p. 487. https://doi.org/10.3390/polym15030487
22. Faingol'd, E.E., Saratovskikh, S.L., Panin, A.N., Babkina, O.N., Zharkov, I.V., Kapasharov, A.T., Lashmanov, N.N., Shilov, G.V., and Bravaya, N.M., *Polyolefins J*., 2023, vol. 10, pp. 205–210. https://doi.org/10.22063/poj.2023.3417.1270
23. ASTM D3900-05a. Standard Test Methods for Rubber-Determination of Ethylene Units in Ethylene-Propylene Copolymers (EPM) and in Ethylene-Propylene-Diene Terpolymers (EPDM) by Infrared Spectrometry, 2010.
24. Cran, M.J. and Bigger, S.W., *Appl. Spectros*., 2003, vol. 57, pp. 928–932. https://doi.org/10.1366/000370203322258887
25. Sobhanmanesh, K. and Hajizadeh, A., *Iranian Polymer J*., 2004, vol. 13, pp. 257–262. https://www.sid.ir/paper/85918/en
26. Ali, A., Moradian, J.M., Naveed, A., Aziz, T., Muhammad, N., Maouche, C., Guo, Y., Yaseen, W., Yassen, M., Haq, F., Hassan, M., Fan, Z., and Guo, L., *Polymers*, 2022, vol. 14, pp. 3239. https://doi.org/10.3390/polym14163239